

Fragility curves for woodframe structures subjected to lateral wind loads

Kyung Ho Lee[†] and David V. Rosowsky[‡]

Zachry Department of Civil Engineering, Texas A&M University, College Station, TX 77843-3136, USA

(Received August 1, 2004, Accepted February 23, 2006)

Abstract. This paper describes a procedure to develop fragility curves for woodframe structures subjected to lateral wind loads. The fragilities are cast in terms of horizontal displacement criteria (maximum drift at the top of the shearwalls). The procedure is illustrated through the development of fragility curves for one and two-story residential woodframe buildings in high wind regions. The structures were analyzed using a monotonic pushover analysis to develop the relationship between displacement and base shear. The base shear values were then transformed to equivalent nominal wind speeds using information on the geometry of the baseline buildings and the wind load equations (and associated parameters) in ASCE 7-02. Displacement vs. equivalent nominal wind speed curves were used to determine the critical wind direction, and Monte Carlo simulation was used along with wind load parameter statistics provided by Ellingwood and Tekie (1999) to construct displacement vs. wind speed curves. Wind speeds corresponding to a presumed limit displacement were used to construct fragility curves. Since the fragilities were fit well using a lognormal CDF and had similar logarithmic standard deviations (ξ), a quick analysis to develop approximate fragilities is possible, and this also is illustrated. Finally, a compound fragility curve, defined as a weighted combination of individual fragilities, is developed.

Keywords: fragility; performance-based design; probability; pushover analysis; shearwall; wind; wood structures.

1. Introduction

The primary objective of structural design codes and standards is to protect (life) safety by preventing structural collapse or failure during rare events in a building's lifetime. While this objective has largely been achieved for buildings in the U.S. subjected to hurricane wind storms, economic losses and social disruption related to hurricane event are still unacceptable (Ellingwood, *et al.* 2004). Recent disasters in the U.S. and elsewhere around the world have highlighted the social, political, and economic ramifications of the traditional view of codes (to prevent structural collapse during rare events), as economic disruptions caused by structural failures have not been deemed acceptable by the public. This has led to efforts to develop performance-based design procedures in which the structural system is designed to meet multiple specific criteria under given

[†] Post-doctoral Researcher, Formerly, Graduate Research Assistant, Department of Civil, Construction, and Environmental Engineering, Oregon State University, Corvallis, OR, 97331, USA

[‡] A.P. and Florence Wiley Chair and Department Head, Corresponding Author, E-mail: rosowsky@tamu.edu

hazard levels. Performance-based engineering is a new paradigm in which the design process is structured to meet performance expectations (limit states) of the building occupants, owner, and the public. Although performance-based seismic design has advanced for some materials and structural types, such as steel and reinforced concrete buildings and bridges, its application to light-frame wood structures remains relatively unexplored. Performance-based seismic engineering concepts for woodframe buildings are starting to be developed (Ellingwood, *et al.* 2004, Rosowsky and Kim 2002a and 2002b). The focus of that work has been on fragility assessments for woodframe structures exposed to seismic hazards using displacement-based criteria.

Many residential low-rise structures are located along the hurricane-prone coastlines of the United States. Most of these are light-frame wood structures. A review of the performance of woodframe buildings after recent hurricanes – Hugo (1989), Andrew (1992), Iniki (1992), and Opal (1995) – has shown that the majority of damage is due to wind and water. Recent studies have developed fragility curves for roof sheathing uplift in low-rise wood structures (Lee and Rosowsky 2005, Ellingwood, *et al.* 2004). However, lateral displacement from wind pressures acting on the walls and roofs in woodframe structures also can result in structural damage, loss of fenestration, and water ingress into the building. In this study, fragility curves are developed for displacement criteria (maximum shearwall drift) considering lateral wind loads. Like the previous studies which focused on roof sheathing, the hazard is still the wind (speed), however the relevant load effect is the sum of the lateral forces acting on the structure rather than (localized) uplift forces. This paper presents a procedure for constructing fragility curves to assess the response of wood shearwalls subjected to lateral wind load. This was accomplished using monotonic pushover analysis of three baseline structures, Monte Carlo simulation, and statistical fitting techniques. The application of fragility curves to the evaluation of a portfolio of structures is illustrated through the construction of a compound fragility curve.

2. Structural analysis

Three baseline woodframe structures were considered. The structures, which have characteristics (roof slope, square footage, construction material, etc.) typical of single-family residential construction in the U.S., are designated TYPE-I, TYPE-II, and TYPE-III in this paper. The basic construction characteristics of these structures were taken (with some modifications) from other sources (NAHB 1997, Kim 2003). Detailed wall characteristics for the TYPE-I and TYPE-II structures were assumed for this study, while those for the TYPE-III structure were able to be taken directly from (Kim 2003). Table 1 summarizes the dimensions and construction details for the three baseline structures. It should be noted that the contributions of nonstructural finish materials (e.g. gypsum wall board, stucco) and partition walls are not considered in this study. Figs. 1(a)-(c) show the detailed shearwall configurations for the TYPE-I, TYPE-II, and TYPE-III structure, respectively.

Monotonic pushover analysis was conducted to develop curves relating base shear to displacement at the top of the shearwall. Two programs, originally developed as part of the CUREE-Caltech Woodframe Project, were used. The program CASHEW (Folz and Filatroult 2001, 2002) was used to evaluate the dynamic response of individual woodframe shearwalls, and the results were then used as input to a subsequent program to analyze complete woodframe structures. CASHEW is a numerical model capable of predicting the load-displacement response of wood shearwalls under quasi-static cyclic loading. With information on shearwall geometry, material properties, and the hysteretic behavior of the individual fasteners, CASHEW can be used to calculate the parameters of

Table 1 Dimensions and construction details for baseline structures

	TYPE-I	TYPE-II	TYPE-III
Plan dimension	28 ft × 40 ft (8.5 m × 12.2 m)	28 ft × 40 ft (8.5 m × 12.2 m)	20 ft × 32 ft (6.1 m × 9.8 m)
No. of stories	1	2	1
height	8 ft (2.44 m)	16 ft (4.88 m)	8 ft (2.44 m)
stud spacing	16 in o.c. (40.6 cm)	16 in o.c. (40.6 cm)	24 in o.c. (61 cm)
stud size	2 in. × 4 in. ⁽³⁾ (50 mm × 100 mm)	2 in. × 4 in. ⁽³⁾ (50 mm × 100 mm)	2 in. × 4 in. ⁽³⁾ (50 mm × 100 mm)
Wall sheathing panel	OSB 3/8 in. (9.5 mm)	OSB 3/8 in. (9.5 mm)	OSB 3/8 in. (9.5 mm)
nail type	8d box nail ⁽¹⁾	8d box nail ⁽¹⁾	Durham spiral nail ⁽²⁾
nail schedule [edge/field]	6 in. / 12 in. (150 mm / 300 mm)	6 in. / 12 in. (150 mm / 300 mm)	6 in. / 12 in. (150 mm / 300 mm)
hold-down	assumed to be designed and installed properly		
Roof type	Gable	Gable	Gable
slope	6:12 (26.6°)	8:12 (33.7°)	4:12 (18.4°)
overhang	12 inch (30.5 cm)	12 inch (30.5 cm)	12 inch (30.5 cm)

⁽¹⁾2^{1/2} in. (63.5 mm) long × 0.113 in. (2.87 mm) diameter

⁽²⁾2 in. (150 mm) long × 0.105 in. (2.67 mm) diameter

⁽³⁾the top-plate and end studs are double members while the sole-plate and interior studs are single members.

an equivalent single degree-of-freedom (SDOF) oscillator for an isolated shearwall. The equivalent SDOF model can be then used for either monotonic or cyclic analysis of the shearwall, or to evaluate shearwall response under an actual or synthetic ground motion record. The SDOF oscillator also can become input information into the program SAWS (Folz and Filtrault 2003) which is used to analyze complete woodframe structures. In the SAWS program, the light-frame structure is composed of two primary components: rigid horizontal diaphragms and nonlinear lateral load-resisting shearwall elements. In the modeling of the structure, it is assumed that both the floor and roof elements have sufficiently high in-plane stiffness to be considered rigid elements. This is a reasonable assumption for typically constructed diaphragms with a planar aspect ratio on the order of 2:1, as supported by experimental results from full-scale diaphragm tests (Phillips, *et al.* 1993). The actual three-dimensional building is degenerated into a two-dimensional planar model using zero-height shearwall elements connected between the diaphragm and the foundation. In this study, the distribution of the lateral load over the height of a structure is assumed to be uniform, a reasonable assumption for low-rise buildings. The SAWS program assigns nodal loads which are applied to the center of mass at each floor level. Fig. 2 shows examples of pushover curves (one for each load direction) for the TYPE-III structure.

3. Wind loads

Once the displacement vs. base shear curve (Fig. 2) is determined, the next step is to convert base shears to equivalent nominal wind speeds in order to determine the critical (weakest) direction for

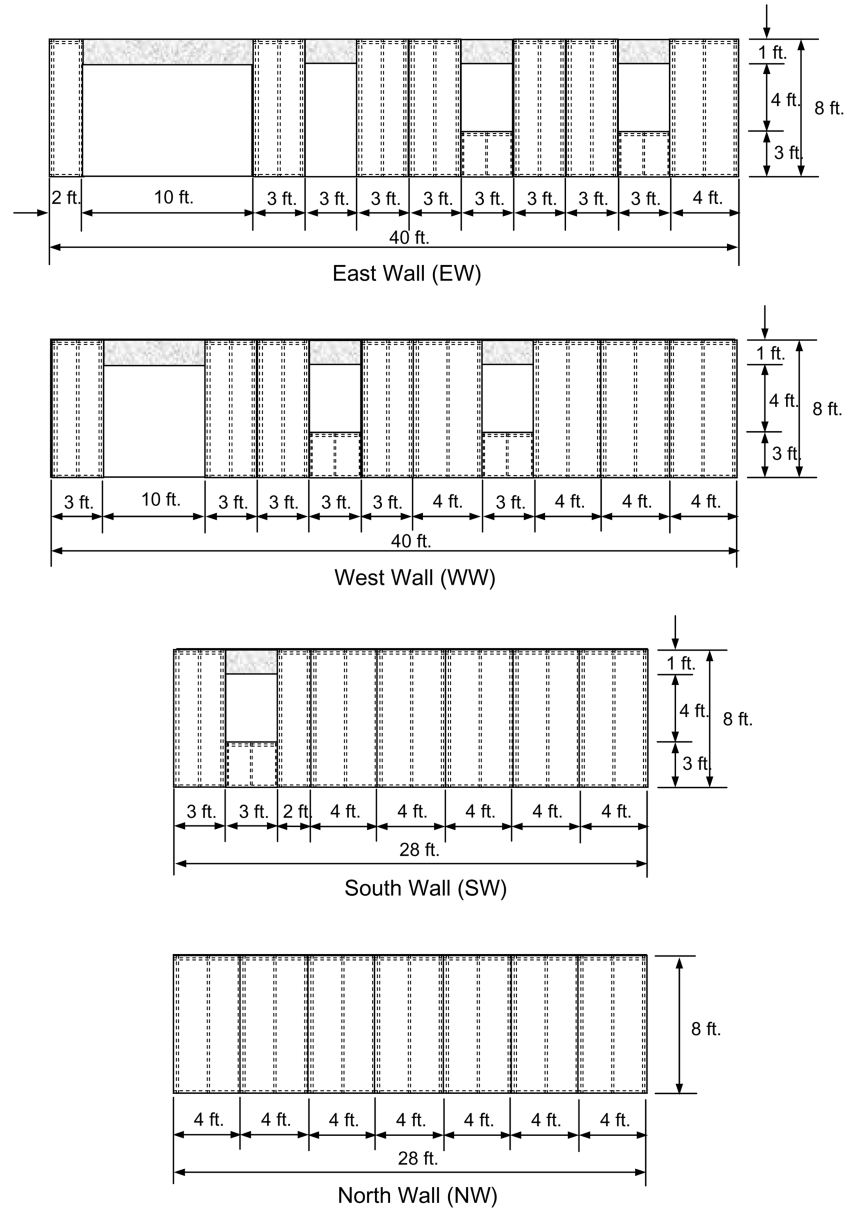
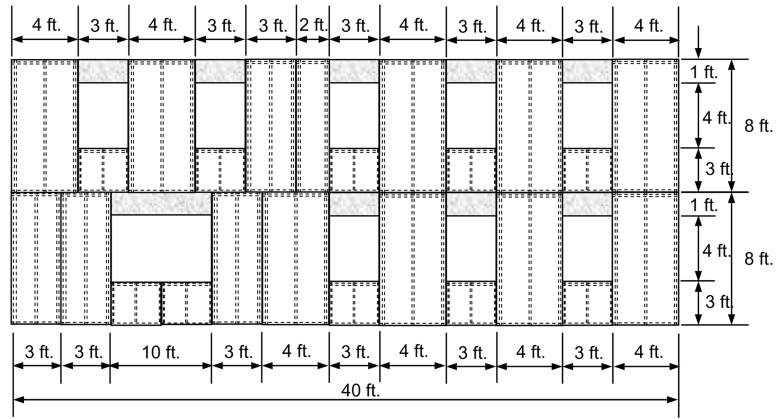


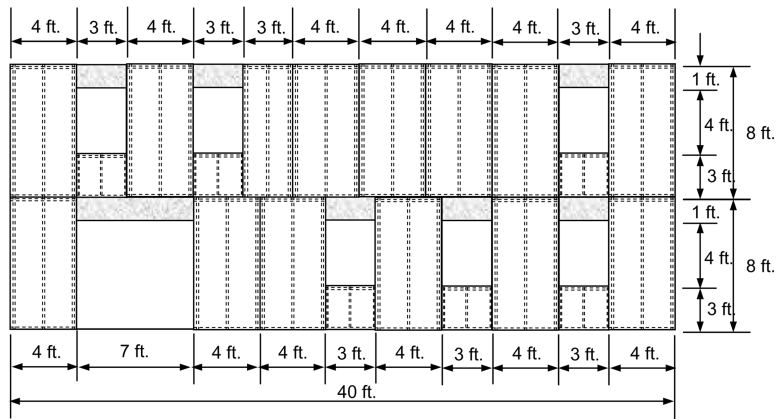
Fig. 1(a) Detailed wall configurations for the TYPE-I house model

the structure. ASCE (2002) provides different external pressure coefficients (GC_{pf}) for different building surfaces (Figs. 6-10 in ASCE 7-02). Therefore, base shears are determined by summing the wind pressures multiplied by their respective projected areas. The procedure for then converting base shear to equivalent wind speed is described in this section.

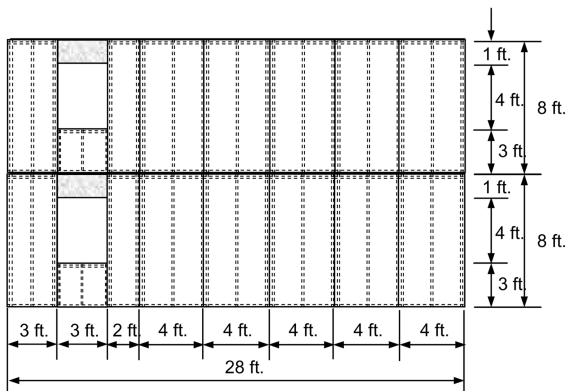
ASCE 7 (2002) defines two types of structural elements subjected to wind load: (1) main wind-force resisting systems (MWFRS), and (2) components and cladding (C&C). Different elements have different effective tributary areas as well as different wind pressure coefficients. A main wind-



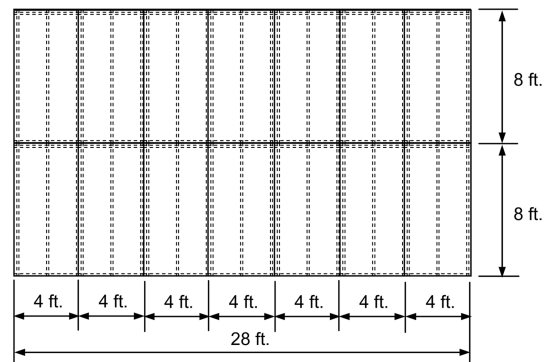
East Wall (EW)



West Wall (WW)



South Wall (SW)



North Wall (NW)

Fig. 1(b) Detailed wall configurations for the TYPE-II house model

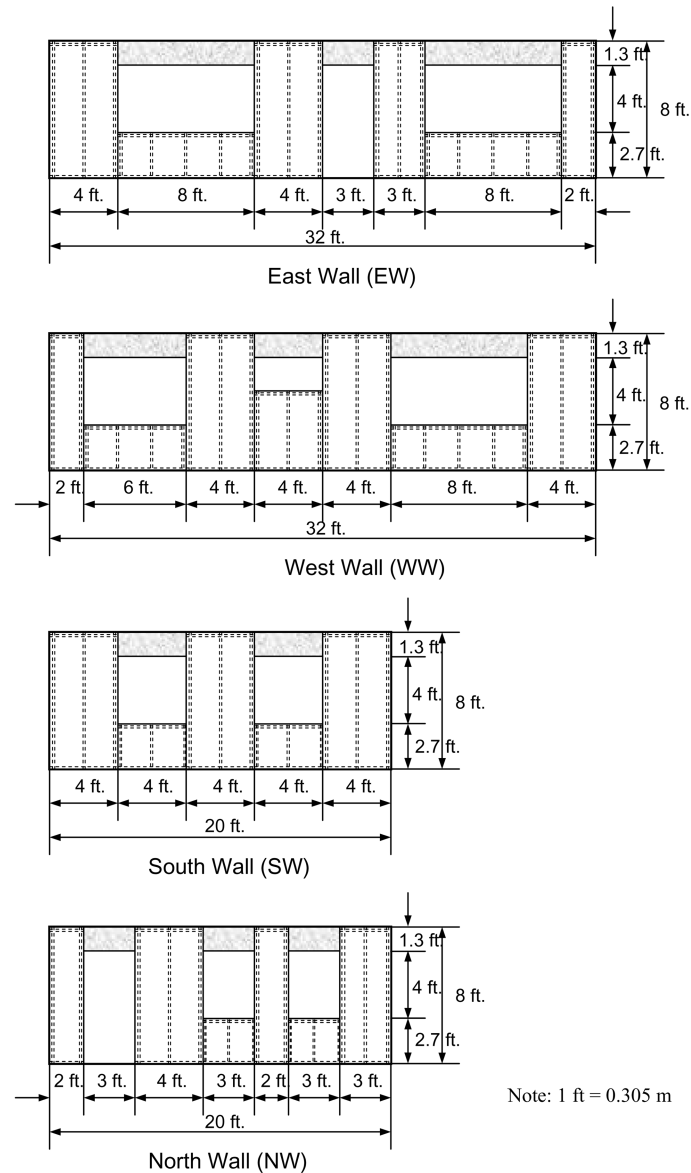


Fig. 1(c) Detailed wall configurations for the TYPE-III house model

force resisting system (MWFRS) is considered an assemblage of structural elements that work together to provide support and stability for the overall structure. Components and cladding (C&C) elements are defined as elements of the building envelope that transfer the load to the main wind-force resisting system. Shearwalls and horizontal diaphragms can be considered main wind-force resisting systems. Therefore, lateral wind pressures acting on the wall and roof in this study were calculated using the MWFRS provisions in ASCE (2002). The wind pressure acting on a main wind-force resisting system for low-rise structures in ASCE (2002) (Eqs. 6-18) can be determined from:

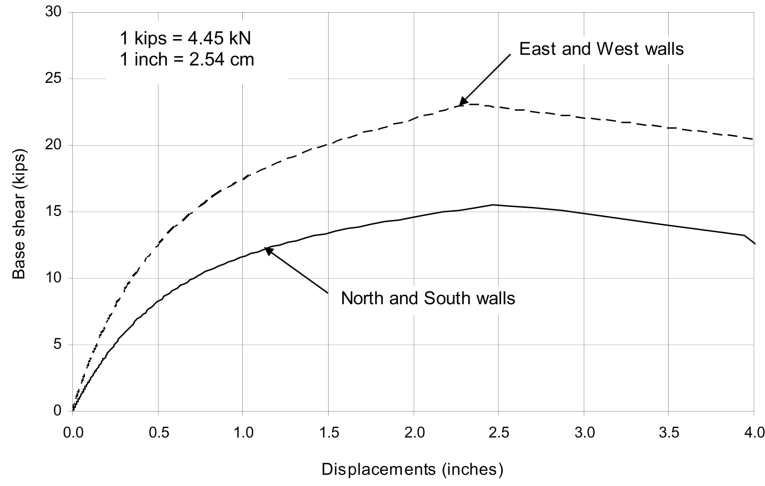


Fig. 2 Pushover curves for Type-III building considering two different load directions

$$W = q_h[(GC_{pf}) - (GC_{pi})] \tag{1}$$

where q_h = velocity pressure evaluated at mean roof height (h), GC_{pf} = product of gust factor and external pressure coefficient, and GC_{pi} = product of gust factor and internal pressure coefficient. The velocity pressure evaluated at height z in ASCE 7-02 (Eqs. 6-15) is given by:

$$q_z = 0.00256K_zK_{zt}K_dV^2I \tag{2}$$

where q_z is velocity pressure (equivalent to q_h) at the mean roof height in units of lb/ft^2 . K_z = the velocity pressure exposure coefficient, K_{zt} = the topographic factor, K_d = the wind directionality factor, V = the basic wind speed (3-second gust wind speed at 33 ft (10 m) in open terrain) in mph, and I = the importance factor. Wind effects on low-rise buildings are characterized for the purpose of design as distributed static loads. The external pressure coefficient, GC_{pf} , varies by wind direction and wall and roof surfaces. The wind pressure can be determined from Eqs. (1) and (2) as:

$$W = 0.00256K_zK_{zt}K_dV^2I[(GC_{pf}) - (GC_{pi})] \tag{3}$$

where, W is a wind pressure in lb/ft^2 . Any internal (compartmental) pressure effects in Eq. (3) are ignored. Therefore, Eq. (3) can be simplified as:

$$W = 0.00256K_zK_{zt}K_dV^2I(GC_{pf}) \tag{4}$$

External pressure coefficient, GC_{pf} , depends on location on the building surface (see Figs. 6-10 in ASCE 7-02). Therefore, Eq. (4) can be presented as a summation of each wind pressures acting on various locations as:

$$W = \sum_{i=1}^n W_{(i)} = \sum_{i=1}^n 0.00256K_zK_{zt}K_dV^2I(GC_{pf}^{(i)}) \tag{5}$$

where $GC_{pf}^{(i)}$ = external pressure coefficient at location i . In the case of low-rise structures, V , K_z , K_{zt} , K_d and I do not depend on the specific location i . The total base shear for a structure can be expressed as the summation of wind pressures multiplied by the corresponding projected areas.

$$\begin{aligned} B &= \sum_{i=1}^n [W_{(i)} \times A_{(i)}] = \sum_{i=1}^n [0.00256 K_z K_{zt} K_d V^2 I (GC_{pf}^{(i)}) \times A_{(i)}] \\ &= 0.00256 K_z K_{zt} K_d V^2 I \sum_{i=1}^n [(GC_{pf}^{(i)}) \times A_{(i)}] \end{aligned} \quad (6)$$

where B = base shear (lbs), $W_{(i)}$ = wind pressure acting on surface i (psf), and $A_{(i)}$ = projected area (ft^2) of surface i . The equivalent wind speed corresponding to this value of base shear can then be obtained as:

$$V = \left(\frac{B}{0.00256 K_z K_{zt} K_d I \sum_{i=1}^n [(GC_{pf}^{(i)}) \times A_{(i)}]} \right)^{\frac{1}{2}} \quad (7)$$

In Eq. (7), equivalent wind speed V is given in units of mph, base shear B in lbs, and area $A_{(i)}$ in square feet. Note that wind pressures acting on the roof surfaces were resolved into horizontal and vertical components, and that both horizontal pressures on the roof and external pressures on the front and back walls were considered in determining the net lateral load on the structure.

4. Lateral wind fragilities

Using pushover curves (displacement vs. base shear), the relation between base shear and wind speed given by Eq. (7), and the nominal wind load parameters in Table 2, displacement vs. equivalent nominal wind speed curves were obtained. Fig. 3 shows the displacements vs. wind speed curves for shearwalls in the different wind directions for the TYPE-III building assuming Exposure C. As shown in Fig. 3, the North and South walls in all three baseline structures performed the worst, and therefore the critical direction of wind loading was the East-West direction. For the one-story baseline buildings, displacement was calculated at the top of the shearwall. For the two-story baseline building, the critical displacement was taken as the largest of: (1) drift at the top of the first story; (2) interstory drift; and (3) drift at the top of the second story (roof diaphragm level), and the appropriate heights were used to evaluate drift ratios per FEMA 356 (FEMA 2000a, b). In general, the drifts at the top of the structure governed. Therefore, displacement at the top of the second story (roof diaphragm level) relative to the ground (i.e. full building height) was considered when evaluating drift performance. Two displacement limit states were considered, namely drift ratios (ratios of lateral displacement to wall height) of 1% and 2%. These are the drift limits suggested by FEMA 356 for woodframe shearwalls corresponding to the IO (immediate occupancy) and LS (life safety) performance levels, respectively. While these drift limits were developed for seismic design, they are tied to performance requirements (occupancy, life safety) that are also relevant for structures under wind

Table 2 Statistics for wind load parameters (based on work by Ellingwood and Tekie 1999)

Wind load factors	Categories	Nominal	Mean-to-nominal (mean)	COV	CDF
Velocity pressure	Exp B	0.70	1.01 (0.71)	0.19	Normal
	Exp C	0.85	0.96 (0.82)	0.14	
	Exp D	1.03	0.96 (0.99)	0.14	
Directionality	MWFRS	0.85	1.01 (0.86)	0.125	Normal
Topographic	-	-	deterministic (= 1.0)		
Importance	-	-	deterministic (= 1.0)		
External pressure	zones 1,2,3,4	(1)	0.86	0.18	Normal
	zones 1E,2E,3E,4E	(1)	0.80	0.18	Normal

⁽¹⁾from Figs. 6-10 in ASCE 7-02

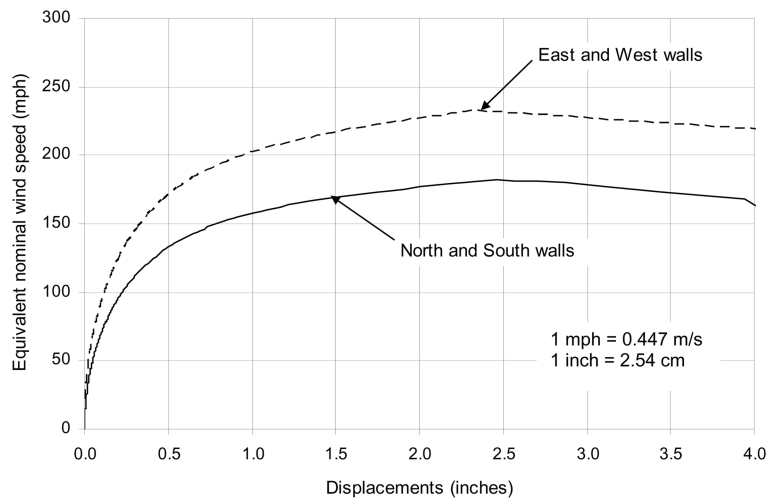


Fig. 3 Equivalent wind speed pushover curves for Type-III building considering two different wind directions

loading³. Fig. 3 was developed using nominal wind load parameters provided by ASCE 7-02 (ASCE 2002). Fig. 4 shows curves developed using Monte Carlo simulation and the wind load statistics in Table 2. The fragility of a structural system can modeled using a lognormal distribution,

$$Fr(x) = \Phi \left[\frac{\ln(x) - \lambda}{\xi} \right] \tag{8}$$

³Lateral drift is only one possibly relevant limit state for structures under high wind loading. Others include roof covering/sheathing removal, failure of doors or windows, rigid body rotation of the roof off the walls, or movement of the entire structure off the foundation. The degree to which each of these limit states may be significant depends on the amount of connections, fasteners, or anchorage. Only the lateral drift limit state is considered here.

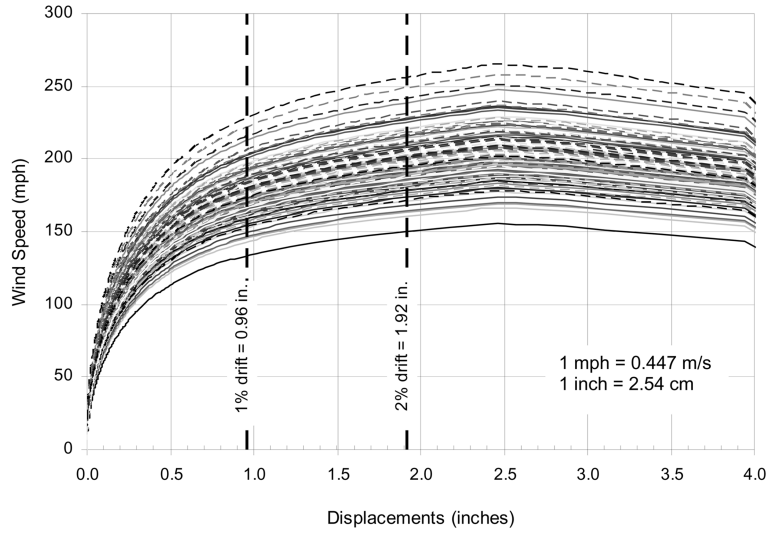


Fig. 4 Equivalent wind speed pushover curves considering random wind load [Type-III building, Exposure C, with directionality factor]

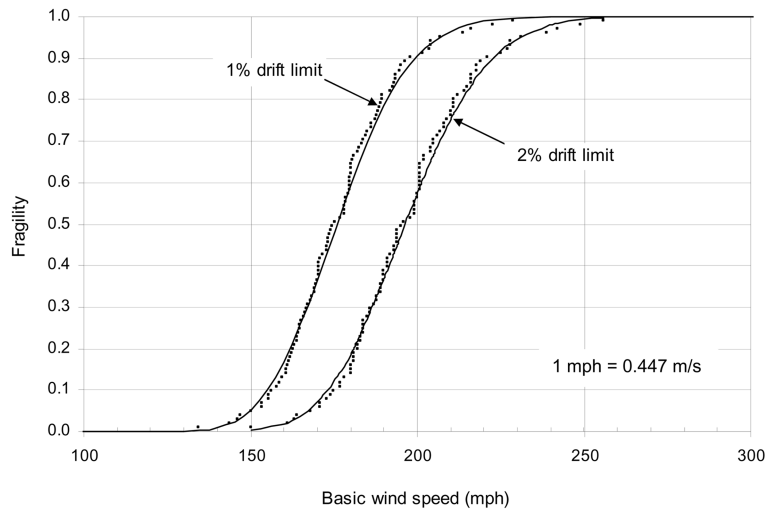


Fig. 5 Lognormal-fitted fragility curves for different displacement limits [TYPE-III building, Exposure C, with directionality factor]

in which $\Phi[\cdot]$ = standard normal cumulative distribution function, λ = logarithmic median of variable x , and ξ = logarithmic standard deviation of variable x . Using the wind speeds at each displacement limit, lateral wind load fragilities (conditional probabilities of failure) were developed and fit using a lognormal distribution as shown in Fig. 5. Figs. 4 and 5 were developed for the TYPE-III structure assuming Exposure C and including the wind directionality factor as a random variable (mean = 0.86, COV = 0.125). ASCE 7-02 provides a wind directionality factor of 0.85 (for MWFRS in ordinary buildings) to account for two effects: (1) the reduced probability of maximum winds

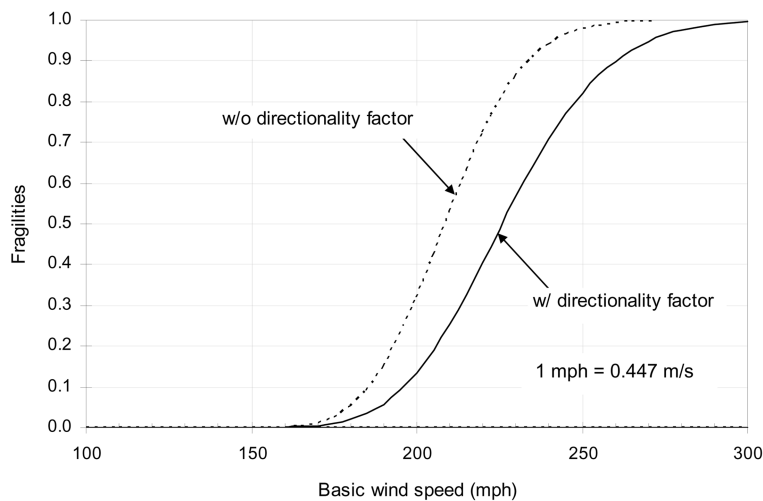


Fig. 6 Fragility comparison with and without wind directionality factor [TYPE-I building, 1% drift limit, Exposure B]

coming from any given direction, and (2) the reduced probability of the maximum pressure coefficient occurring for any given wind direction (ASCE 2002). Two types of fragilities were developed in this study: one that includes the wind directionality effect (directionality factor modeled as a random variable) and one that does not (no directionality factor). Fig. 6 shows a comparison of fragilities with and without consideration of wind directionality. Table 3 presents a complete set of lognormal parameters for the fragility curves considering all cases.

Since the variation in the dispersion parameter (ξ) in Table 3 is small, the lateral wind load fragilities can be obtained directly and more easily if we determine the wind speed corresponding to the median fragility, $Fr(x)=0.5$. The wind speed corresponding to the median fragility can be determined using Eq. (7), the median values of wind load statistics in Table 2, and the base shear corresponding to the drift limit (determined from the deterministic pushover analysis). Using Eq. (7) and the median values of wind load parameters in Eq. (7), the median wind speeds at the 1% and 2% drift limits were determined to be 175 mph (78.2 m/s) and 194 mph (86.7 m/s), respectively. The mean of the logarithmic standard deviation ξ (for the case including the wind directionality factor) in Table 3 is 0.11. Therefore, quick estimations of the lognormal fragility parameters would be $\lambda = \ln(175) = 5.16$ and $\xi = 0.11$ for the 1% drift limit, and $\lambda = \ln(194) = 5.27$ and $\xi = 0.11$ for the 2% drift limit. Using these parameters, one obtains estimates of the fragility curves without the need for simulation or statistical fitting techniques. Fig. 7 shows that fragilities constructed using the simplified analysis are very close to those developed using simulation.

5. Compound fragility

Fragility curves also have application to pre-disaster vulnerability assessment as well as post-disaster condition assessment. Some of these potential applications have been discussed elsewhere (Rosowsky and Ellingwood 2002). It may be possible, for example, to use fragility curves such as those developed in this paper, to evaluate a single aggregate fragility that applies to a building inventory (portfolio), rather than a single structure. The implications to disaster planners as well as

Table 3 Lognormal parameters for lateral wind fragilities determined by simulation

Drift limit	Structure	Exposure	with directionality factor		without directionality factor	
			λ	ξ	λ	ξ
1%	TYPE-I	B	5.43	0.12	5.35	0.11
		C	5.35	0.10	5.28	0.08
		D	5.25	0.11	5.18	0.08
	TYPE-II ⁽¹⁾	B	5.14	0.12	5.16	0.11
		C	5.06	0.10	5.08	0.08
		D	4.97	0.10	4.99	0.08
	TYPE-III	B	5.25	0.13	5.16	0.12
		C	5.17	0.10	5.10	0.09
		D	5.08	0.12	5.00	0.09
2%	TYPE-I	B	5.52	0.12	5.45	0.11
		C	5.45	0.10	5.37	0.08
		D	5.36	0.11	5.27	0.09
	TYPE-III	B	5.36	0.13	5.29	0.12
		C	5.28	0.10	5.21	0.09
		D	5.19	0.11	5.12	0.09

⁽¹⁾Note: the TYPE-II structure failed before the 2% drift limit was reached.

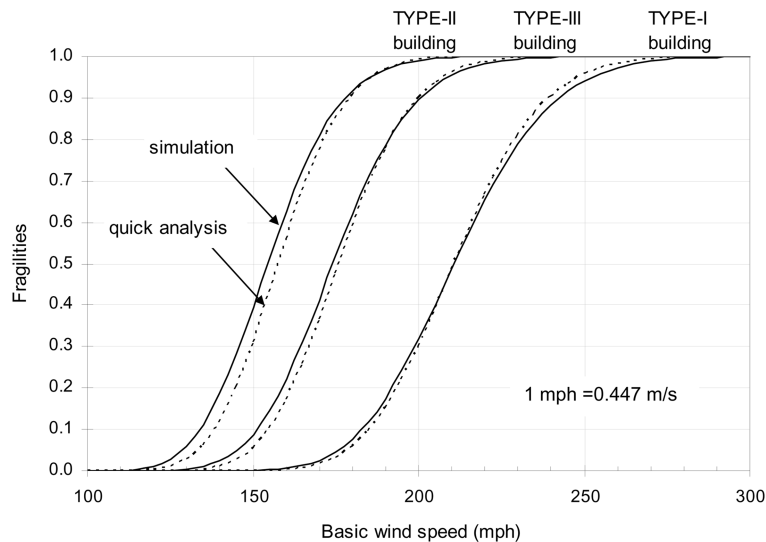


Fig. 7 Comparison of fragilities using the simulation and the quick analysis [1% drift limit, Exposure C, with directionality factor]

the insurance industry are obvious. Consider a portfolio of structures that can be divided into n classes of buildings (types, ages, materials, condition, etc.) where the relative percentage of class i is given by a weighting term w_i . A *compound fragility* $Fr^{(C)}(x)$ (for the portfolio of structures) can be

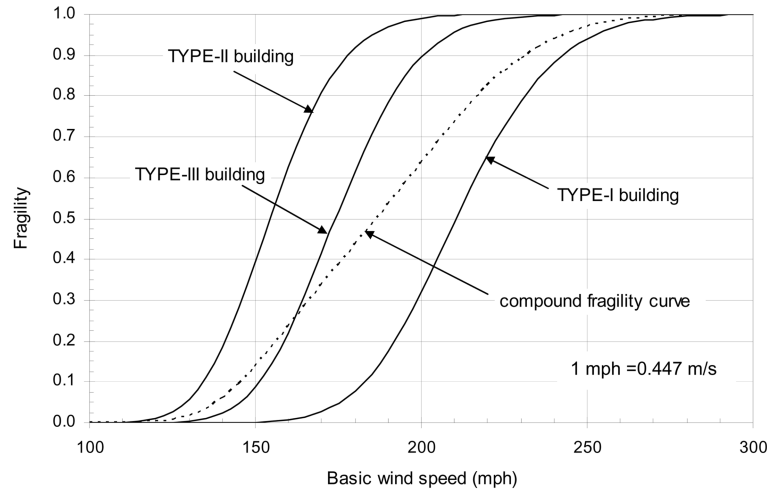


Fig. 8 Example of compound fragility curve [1% drift limit, Exposure C, with directionality factor] [Example for TYPE-I (50%), TYPE-II (30%), and TYPE III (20%)]

computed as:

$$Fr^{(C)}(x) = \sum_{i=1}^n w_i Fr^{(i)}(x) \quad (9)$$

where w_i = weight for structure type i , and $Fr^{(i)}(x)$ = individual fragility for structure type i . Assuming all of the individual fragilities can be described by a lognormal distribution, Eq. (9) can be written:

$$Fr^{(C)}(x) = \sum_{i=1}^n w_i \Phi\left(\frac{\ln(x) - \lambda_{R,i}}{\xi_{R,i}}\right) \quad (10)$$

where $\Phi(\cdot)$ = standard normal CDF, $\lambda_{R,i}$ = logarithmic median of capacity R of structure i , and $\xi_{R,i}$ = logarithmic standard deviation of capacity R of structure i . Fig. 8 shows the compound fragility (considering the 1% drift limit) computed using Eq. (10) for a portfolio of structures consisting of 50% TYPE-I buildings, 30% TYPE-II buildings, and 20% TYPE-III buildings. All structures are assumed to be located in Exposure C. The individual structure fragilities, constructed using the simplified procedure, also are shown in Fig. 8.

6. Conclusions

This study developed fragility curves for low-rise woodframe structures subjected to lateral wind loads. To accomplish this, three baseline structures were analyzed using a monotonic pushover analysis procedure that resulted in displacement vs. base shear curves. The base shears were then transformed to equivalent nominal wind speeds using configuration information of the baseline buildings and the wind load equations in ASCE 7-02. The displacement vs. equivalent nominal wind speed curves were used to determine the critical wind direction. Monte Carlo simulation was used along with statistics for wind load parameters to construct displacement vs. wind speed curves,

and wind speeds corresponding to different displacement limits were then plotted to form fragility curves. The lateral wind fragility curves were well fit by a lognormal CDF. Since the range of lognormal dispersion parameter ξ was small, approximate fragility curves also were able to be developed using the median value of wind speed at each drift limit and the average value of ξ . This approach does not require numerical simulation or statistical fitting techniques. Finally, a procedure was described for constructing a compound fragility which could be used to evaluate expected performance of an inventory of buildings.

The fragility methodology described herein can be used to develop performance-based design guidelines for woodframe structures in high wind regions as well as provide information on which to base structural safety and expected structural or economic loss assessments. Fragilities such as those presented here also can be convolved with wind hazard curves to evaluate probabilities of failure (in this case, excessive lateral drift) considering different performance levels.

References

- ASCE (2002), "Minimum design loads for buildings and other structures, Standard ASCE 7-02", *Structural Engineering Institute of the American Society of Civil Engineers*, Reston, VA.
- Durham, J.P. (1998), "Seismic response of wood shearwalls with oversized oriented strand board panels", MASc Thesis, University of British Columbia, Vancouver, Canada.
- Ellingwood, B.R. and Tekie, P.B. (1999), "Wind load statistics for probability-based structural design", *J. Struct. Eng.*, ASCE, **125**(4), 453-463.
- Ellingwood, B.R., Rosowsky, D.V., Li, Y. and Kim, J.H. (2004), "Fragility assessment of light-frame wood construction subjected to wind and earthquake hazards", *J. Struct. Eng.*, ASCE, **130**(12), 1921-1930.
- FEMA (2000a), "Prestandard and commentary for the seismic rehabilitation of buildings", *Federal Emergency Management Agency*, Washington, DC.
- FEMA (2000b), "Global topics report on the prestandard and commentary for the seismic rehabilitation of buildings", *Federal Emergency Management Agency*, Washington, DC.
- Folz, B. and Filiatrault, A. (2000), "CASHEW-Version 1.0: A computer program for cyclic analysis of wood shear walls", CUREE Publication No. W-08, Consortium of Universities for Research in Earthquake Engineering, Richmond, CA.
- Folz, B. and Filiatrault, A. (2003), "SAWS-A computer program for seismic analysis of woodframe structures", CUREE Publication No. W-21, Consortium of Universities for Research in Earthquake Engineering, Richmond, CA.
- Kim, J.H. (2003), "Performance-based seismic design of light-frame shearwalls", Ph.D. Dissertation, Department of Civil, Construction, and Environmental Engineering, Oregon State University, Corvallis, OR.
- Lee, K.H. and Rosowsky, D.V. (2005), "Fragility assessment for roof sheathing failure in high wind regions", *Eng. Struct.*, **27**, 857-868.
- Lee, K.H. (2004), "Site-specific hazards and load models for probability-based design", Ph.D. dissertation, Department of Civil, Construction, and Environmental Engineering, Oregon State University, Corvallis, OR.
- NAHB (1997), "Housing affordability through design efficiency program", NAHB Research Center, Inc., Upper Marlboro, MD.
- Rosowsky, D.V. and Ellingwood, B.R. (2002), "Performance-based engineering of wood frame housing: A fragility analysis methodology", *J. Struct. Eng.*, ASCE, **128**(1), 32-38.
- Philips, Y.L., Itani, R.Y. and McLean, D.L. (1993), "Lateral load sharing by diaphragms in wood-frame buildings", *J. Struct. Eng.*, ASCE, **119**(5), 1556-1571.